

Generalized Spectral Inversion Techniques Benchmark (GITEC)

WORK PACKAGE 3 - GROUND MOTION



AUTHORS		REVIEW		APPROVAL	
Name	Date	Name	Date	Name	Date
<i>Hussein SHIBLE</i>	2019/05/03	Ian Main  Christophe MARTIN	2021/01/05 2021/02/21	<i>Fabrice Hollender</i>  Public-access <input checked="" type="radio"/> SIGMA-2 restricted <input type="radio"/>	2022/11/29 2022/.../

DISSEMINATION: This document must not be distributed to any person, institution or company other than members of SIGMA-2 steering and scientific committees, except under written formal permission of SIGMA-2 steering committee.

	<p style="text-align: center;">Research and Development Program on Seismic Ground Motion</p>	<p>Réf : SIGMA2-2019-D3-030/1</p>
		<p>Version : 1</p>

Document history

DATE	VERSION	COMMENTS
<i>YYYY/MM/DD</i>	<i>0</i>	

Executive summary

Generalized inversion techniques (GIT) have become popular techniques for determining ground motion parameters (source, attenuation, and site-responses), particularly in low-to-moderate seismicity regions. Indeed, it seems that GIT can potentially provide reliable site response estimates, even at sites where few recordings are available, as well as valuable information about source features (magnitudes, corner frequencies, stress drops...) and regional attenuation characteristics. Recent advances have been made in GIT, different approaches and alternative basic hypotheses are followed by different research groups, such as the application of “non-parametric” (e.g. Bindi et al., 2017, Castro et al., 1990) and “parametric” (e.g. Drouet et al., 2010, Edwards et al., 2008) inversion schemes. In this context, some scientific questions rise. Depending on the final scope of GIT, what can be the optimal dataset configuration and the best inversion strategy? What is the impact of the different assumptions and implementations on the reliability of the results? What is the dependence of the results on the chosen reference conditions? Is it possible to quantify the associated epistemic uncertainties? In this text, and within the framework of SIGMA-2 program, we have the interest to compare the different approaches available as to improve the understanding of the impact of different GIT implementations in different applications. To fulfill the objective, a methodological benchmark among different generalized spectral inversion methods and dataset configurations has been performed: a French regional sparse dataset, an Italian national dense dataset and a Japanese wide dataset. The results on each dataset is illustrated and compared showing the discrepancies resulting from each GIT scheme. Despite unifying the initial conditions such as reference distances and sites (expecting to reduce the differences in results), significant level of inter-methods variability was observed and quantified. At the end, some observations and remarks are illustrated comparing the different datasets/methods considered.

Table des matières

Document history	2
Executive summary	2
Introduction	4
1. GIT Methodologies and schemes included in the benchmark:	6
2. The datasets considered:	8
3. How to compare results from parametric and non-parametric approaches	11
4. Methods check with a simple synthetic dataset (Sanity check)	12
5. Results on real datasets:	14
5.1. Choice of the reference sites in each dataset:	14
5.2. French dataset results:	14
5.3. Central Italy dataset results:	17
5.4. Japanese dataset results:	20
6. Inter-methods variability assessment	22
6.1. French dataset case :	22
6.2. Central Italy dataset case :	24
6.3. Japanese dataset case:	25
7. Summary and conclusions:	27
8. Future perspectives:	28
Acknowledgements	29
References	29

	<p>Research and Development Program on Seismic Ground Motion</p>	<p>Réf : SIGMA2-2019-D3-030/1</p>
		<p>Version : 1</p>

Introduction

Seismic waves initiate from faults and ruptures in the Earth crust and propagate from its source, through different paths, to reach the surface affecting building structures and other installations above or below Earth surface. The observed strong ground motions on the surface are deeply affected by several factors such as the rupture nature (source effects), the way the waves propagate to reach a specific site (path effects) and the amplification of motion amplitudes that occurs while propagating through certain geological structures to reach the surface (site effects). After several destructive earthquakes through the years (Mexico 1985, Kobe 1995, Tōhoku 2011), accurate evaluation of strong ground motion factors have become a necessity and a crucial step for quantitative predictions of future strong earthquakes for special structures such as high-rise buildings and nuclear installations.

Seismic hazard assessment studies are carried out generally to predict the intensity of ground shaking in a given region through regression studies on empirically recorded data to develop ground motion prediction equations (GMPEs). As in some regions where there is lack of sufficient instrumentation and earthquake coverage or in the case of low-to-moderate seismicity regions, stochastic simulations of ground motion can be aiding to develop ground motions predictions. In this case, a careful estimation of the key physical source and attenuation parameters used in stochastic simulations as well as site amplifications is needed. To add, site-specific seismic hazard assessment is a general need that requires the knowledge of site amplifications. These site amplifications are generally assessed through site characterizations that is not always possible or available. In the aim to evaluate ground motion key factors, generalized inversion techniques (GIT), which use Fourier spectra of recorded data, serve a beneficial tool.

This technique was first introduced by (Andrews, 1986) and is based on the assumption of separation of the Fourier spectrum of a recorded seismic signal into source, path and site factors. Generalized inversion techniques have been used in detailed studies to explore the frequency-dependent attenuation characteristics in addition to the main source parameters and the site effects. For example, several studies using GIT approaches (Parolai et al., 2004; Bindi et al., 2006) have focused on attenuation showing that in the short source-to-station distances high attenuation can be inferred from the upper crust, while longer source-to-station distances have suggested lower attenuation characteristics of the deeper crustal layers. GIT also offers the advantage to determine site responses as an alternative method to the commonly used Standard Spectral Ratios method or SSR (Borcherdt, 1970) and the Horizontal-to-Vertical Spectral ratio or HVSR (Field and Jacob, 1995; Bonilla et al., 1997; Parolai et al., 2004).

Several studies on site effects estimations from the different possible methods have shown that HVSR may imply an underestimation of the site amplification due to the possibility that vertical components of ground motions may not be exactly “amplification-free” components (Castro et al. (2004), Kurtulmuş et al. (2015)). In addition, numerical simulations of ground motion to determine the site responses generally use a high-resolution shear-wave velocity (V_s) profiles up to a limited soil depth, which may not reflect sufficiently the near surface conditions of the site. Hence, these numerical simulations does not seem to be always providing a proper estimate of the amplification in a given site condition. From this perspective, GIT suggested more reliable empirical estimates of site amplifications as they result simply from the separation of Fourier spectra from the different contributions of source and path effects while there is not any assumption being made on the reference motion that could bias the amplification estimation. In addition, the different studies carried on site

	<p style="text-align: center;">Research and Development Program on Seismic Ground Motion</p>	<p>Réf : SIGMA2-2019-D3-030/1</p>
		<p>Version : 1</p>

effects from generalized inversions showed robust estimations of site amplifications (Parolai et al., 2000). To add, the study of Bindi et al., (2009) and Ameri et al., (2011) on data from central Italy had also provided an indication on the fact that the vertical components of ground motion can be exhibiting some amplifications and the HVSR cannot be always representative of the amplification that horizontal components undergo.

In general, there are two main ways to perform generalized inversions. First, there is the non-parametric approach (Castro et al., 1990; Parolai et al., 2004; Bindi et al., 2006; Pacor et al., 2016) which describes a linear model with some constraints for the unresolved degrees of freedom of the problem. Then the approach can become highly non-linear with parametric approaches which require a priori functional forms for the source and attenuation terms (Hartzell, 1992; Salazar et al., 2007; Drouet et al., 2008; Edwards et al., 2008). As displayed, these GIT approaches has become widely used and several researchers through the years have developed different schemes with different assumptions and constraints.

Within the framework of SIGMA program, generalized inversions have used for several purposes. An example of recent application of generalized inversion techniques was in Bora et al., (2015), where they estimated the key parameters to develop adjustable ground motion models using generalized inversions (named as stochastic ground motion simulation techniques in their text). The study proposed a spectral response ground motion model based on an adjustable Fourier amplitude spectrum (FAS) model where the adjusting parameters were stress drops ($\Delta\sigma$), quality factor Q , and the high-frequency attenuation parameter κ_0 . Also the study by Perron et al., (2017) which focused on the estimations of κ for sites in the Provence area (southern France), tried to compare the Q value obtained from the path term of κ with values obtained from previous studies (including the study of Drouet et al., (2010)) and found significant differences. To add, site effects estimation are of major interest for site-specific hazard assessment studies where an estimation of these site effects can be delivered through generalized inversions. Laurendeau et al., (2018) proposed a methodology for the retrieval of outcropping hard rock motion from surface recordings of earthquakes through a deconvolution procedure using site amplification estimated for each site. The proposed methodology on the KiK-net dataset was possible since theoretical site-responses were calculated using the available shear-wave velocity (V_s) profiles. Looking forward to apply the methodology on European data, generalized inversions is proposed as a solution to deliver an empirical estimation of site amplifications in the lack of enough characterized sites (i.e. available V_s -profiles). Based on these present and future actions within SIGMA, an interest in comparing the different GIT approaches and methods was found motivating to create an international benchmark on the different possible implementations of these techniques to investigate the performance of the different methodologies and to determine the best ways and aspects of using such inversion techniques. In addition, as such ground motion parameters resulting from generalized inversions are being used in a way or another in ground motion predictions, it was important to think about the uncertainty associated with these parameters.

For these interests, “GITEC” (an international benchmark on generalized inversions) was established based on the idea of performing several inversions with multiple GIT schemes on different datasets as well as addressing the possible differences from different approaches on the same dataset. The main scope of the GITEC was to compare and improve the knowledge on the performance of different generalized spectral inversion methods and hypotheses used for estimating ground motion parameters considering the different dataset configurations.

	Research and Development Program on Seismic Ground Motion	Réf : SIGMA2-2019-D3-030/1 Version : 1
---	--	---

The “methodological benchmark” GITEC was expected to serve several broad goals:

- First, the presence of different implementations of the inversion schemes (i.e. parametric and non-parametric) it is important to investigate for the pros and cons of each approach depending on the dataset characteristics considered (dataset geometry, configuration, etc...).
- Exploration of dependence of the results on the assumptions and reference conditions or strategies followed to solve the trade-offs.
- Investigation of the predictive power of each inversion scheme through considering synthetic dataset.
- Several inversion methods applied on the same dataset, allowed us to address the estimation of the epistemic uncertainties on the inverted terms and predicted parameters. However, what is estimated in this work can be more considered as the inter-methods variability, which could be interpreted as a lower bound of the epistemic uncertainty.

The work presented in this text, describes the results obtained from generalized inversions applied by several teams participating in the benchmark. The inversions were distributed mainly on three real datasets that had already been published and used in several studies with slight modifications. An additional synthetic dataset was proposed to check inversion methods and eliminate code problems. Comparing the results from different approaches helped to identify differences in results and thus have an estimation of the observed variability in the results in each of the considered datasets.

1. GIT Methodologies and schemes included in the benchmark:

Generalized inversion schemes initiate from the principle of separation of the amplitude spectrum of ground motion as follows:

$$FAS_{ij}(f) = E_j(f) \cdot P_{ij}(r, f) \cdot S_i(f) \quad (1)$$

where FAS_{ij} is the observed Fourier amplitude spectrum at a given site for a given event, $E_j(f)$ is the source function for a given event j , $P_{ij}(f)$ is the path contribution upon an event j at a given site i , and $S_i(f)$ is the site response term for site i . Each of these terms are assumed independent of each other for a given spectrum. Applying the logarithm on (1), we get the linearized equation as follows:

$$\log_{10}(FAS_{ij}(f)) = \log_{10}(E_j(f)) + \log_{10}(A_{ij}(r, f)) + \log_{10}(S_i(f)) \quad (2)$$

Equation (2) provides a system of linear equations of the form $A \cdot x = b$, where b is the data vector, x is the solution of the system and A describes the system matrix. Following (Andrews, 1986), an undetermined degree of freedom needs to be solved often by the constraining the site response of one or several site, known by their rock conditions or non-amplifying response. The inversion scheme can be implemented in a non-parametric or a parametric way where a priori assumptions can differ. For instance, in a non-parametric approach the attenuation term $A(r, f)$ is considered to be a simple function of distance for each frequency while for the parametric approach an analytic attenuation model along the travel path is considered. The non-parametric approach attenuation is considered to be including all attenuation effects and is referenced to 1 at a given distance called the ‘reference distance’ or ‘ R_{ref} ’. On the other hand, source terms are obtained with no prior assumption on the model in a non-parametric approach, while parametric schemes try to fit a source model, most often

the Brune (1970) omega-2 model. However, it is worth mentioning that the non-parametric inversion schemes assume that their resulting source spectra are shifted to the reference distance R_{ref} as a consequence of the attenuation constraint (i.e. $A(r = R_{ref}, f) = 1$).

The participating methods in the benchmark are summarized in Table 1. Trying to assess the impact of the mentioned different assumptions and constraints, our GITEC benchmark included several inversion schemes that can be classified into three main categories:

- 1- The full non-parametric inversion schemes where all resulting terms are explicit functions of frequency. These inversions can be done through either a single-simultaneous inversion (1-step inversion) or a 2-step inversion.
- 2- The full parametric inversion schemes where source and attenuation contributions are predefined models.
- 3- The semi-parametric (or partially non-parametric) inversion schemes, where only one of the terms is parametrized, e.g. parametrizing the attenuation model but keeping the source spectra as non-parametric curves.

For non-parametric approaches, one GIT scheme included in the benchmark were the 1-step approach developed and used in several investigations: (Bindi et al., 2006, Oth et al., 2008, Bindi et al., 2017). The inversion results corresponding to this inversion scheme hereafter are labelled as ‘01’. To add, another version of the non-parametric GIT but with a 2-step approach was considered (Klin et al., 2017), which determines the attenuation in a first step then resolves the system for the source and site effects. The corresponding inversion results are labelled by ‘02’.

For parametric GIT schemes, the method of Drouet et al., (2010) was considered which models the Fourier spectra of ground motion for the source and attenuation effects (labelled as ‘04’). In addition, another version of the same approach of Drouet et al (2010) was also considered (Grendas et al., 2018), labelled ‘06’. Finally, for parametric GIT, the method of Edwards et al., (2008) was employed in the benchmark, and the corresponding results were labelled by ‘07’. The latter parametric GIT methods model the Fourier spectra of ground motion in a similar way for the source (brune’s model), attenuation (homogenous frequency-dependent Q model with a geometrical spreading factor), and site frequency-dependent amplification.

For semi-parametric approaches, the method of Nakano et al., (2015) was used. This method mainly parametrizes the attenuation with a Q model and frequency dependent geometrical spreading factor and keeps the source and site effects as non-parametric curves. The corresponding results are labelled as ‘05’.

Table 1: table summarizing participating methods.

Inversion Method	Performing Teams	Affiliation	scheme	Abbreviation	Color code
Bindi et al., (2017) / (Oth et al., 2011)	Adrien Oth / Dino Bindi	ECGS, Luxembourg /GFZ Potsdam	Non-parametric (1- step inversion)	01	
Klin et al., (2018)	Peter Klin	OGS, Trieste, Italy	Non-parametric (2- step inversion)	02	

	Research and Development Program on Seismic Ground Motion	Réf : SIGMA2-2019-D3-030/1
		Version : 1

Inversion Method	Performing Teams	Affiliation	scheme	Abbreviation	Color code
Castro et al., (1990) ¹	Raul Castro	CICESE, Mexico	Non-parametric	03	
Drouet et al., (2008)	Hussein Shible	CEA-Cadarache, France	parametric	04	—
Nakano et al., (2015)	Hiroshi Kawaze	Kyoto University, Japan	semi-parametric	05	—
Grendas et al., (2018)	Ioannis Grendas	ITSAK, Greece	parametric	06	—
Edwards et al., (2008)	Ben Edwards	University of Liverpool, England	parametric	07	—

2. The datasets considered:

To investigate the functionality of the different GIT schemes with respect to the different possible characteristics of datasets, several datasets were considered. To investigate the impact on GIT results due to the fact that datasets may exhibit different configurations and characteristics, GITEC aimed to perform inversions on different datasets as follows:

- One dense national dataset (such as the data from the KiK-net/K-net networks).
- A very dense local dataset (example of the central Italy data).
- A regional sparse dataset (example of the RAP dataset in the Alps region).
- Synthetic datasets that would play a control role in the inversion results.

Datasets from previous works and publications were considered in this GIT benchmark with some updates and selections. First, a subset the Japanese dense national network data (Figure 1) used in (Nakano et al., 2015) was chosen, which consists 1541 sites in total (between K-NET, KiK-net and JMA Shindokei network sites) and covers events between 1996/01/11 and 2016/12/28 (341 events) which were also divided into different event types according to their source nature. This dataset contains the magnitude range of events $M_{JMA} > 4.0$ (where M_{JMA} is a magnitude widely used in Japan and is accurate enough to be considered as the moment magnitude for GIT studies); crustal earthquakes with sources depths < 30 km; hypocentral distances $R_{ij} < 200$ km.

1. This results of inversions of Castro et al.,(1990) method were not displayed in this deliverable for verification reasons.

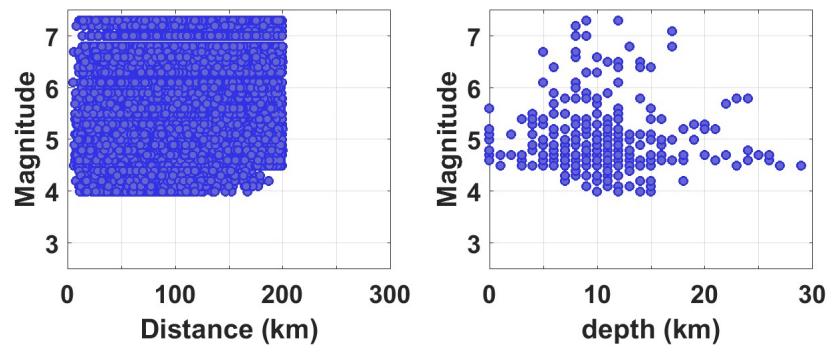


Figure 1: Magnitudes M_{JMA} and hypocentral distances for the Japanese datasets used (Nakano et al., 2015) (left). The depth distribution of the events with their Magnitudes M_{JMA} are shown (right).

Secondly, the regional dense dataset in GITEC was the central Italy dataset similar to that considered in the previous investigations (Bindi et al., 2017) and (Pacor et al., 2016), as seen in Figure 2, with some updates and extensions of the dataset. The considered dataset consists of 231 earthquakes recorded by 309 stations which includes the 2009 L’Aquila sequence ($M_w=6.1$) and spans the time period between July 2008 to January 2017. In this dataset the local magnitudes vary in the range 3.0-6.1 mainly concentrated within 3.0-4.5 range, and the hypocentral distances reach up to 140 km. The depth of earthquakes is mainly distributed within 5 to 10 km range.

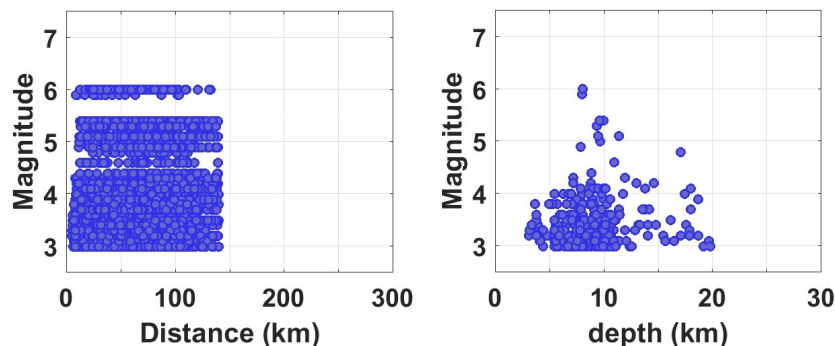


Figure 2 : Magnitude–distance distribution of the data in the central Italy database.

In addition, the French Alps regional sparse datasets used by (Drouet et al., 2010, 2008) was considered. The final dataset consists of 72 earthquakes in the Alps area with hypocentral distances reach up till 250 km. Hypocentral distances of recorded events come from the French national network agency (RéNaSS), and local magnitudes from RéNaSS and LDG (another national French agency). Focal depths are ranging between few kilometers and 10 km. Figure 3 shows the spatial distribution of seismic networks and events in each database considered.

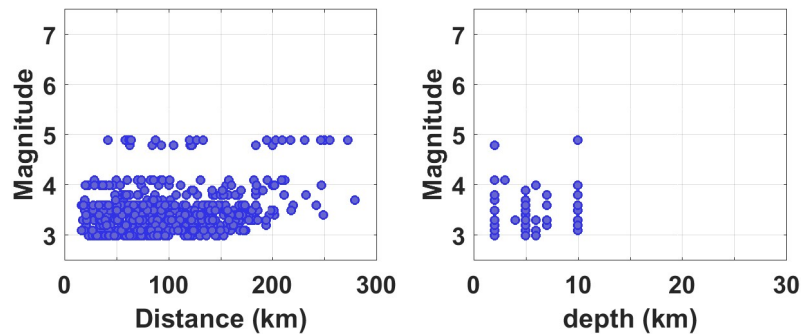


Figure 3 : Magnitude-distance distribution of the data in the Drouet et al., (2010) database.

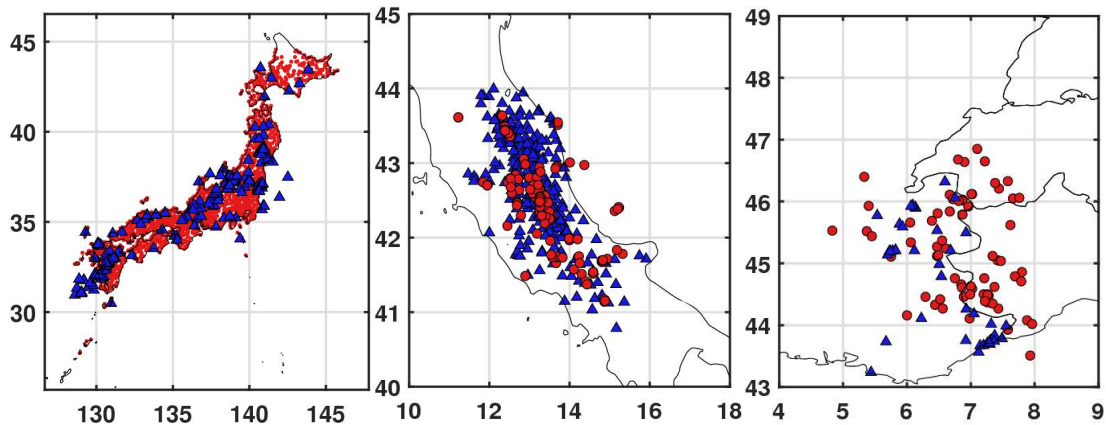


Figure 4 : (a) Path coverage, station locations (triangles) and earthquake epicenters (circles) of each of the considered real datasets (Japan: left, Central Italy: middle, French Alps: right).

Since the primary objective of GITEC was to provide consistent comparisons of the different approaches, it was very essential to provide synthetic datasets that serve as a control of the results, having the opportunity to invert the data obtained from the forward problem. So in addition to real datasets, two synthetic datasets will be addressed too. A very simple synthetic dataset is chosen to start with to ensure consistent comparisons and to be a sort of self-check for each GIT scheme. The results of the different approaches on the simple synthetic dataset is presented in this text. The synthetic data is constructed following the typical formulation of the spectrum of ground-motion (in this case velocity) from an earthquake i recorded at sensor j following equation (1).

The simple synthetic dataset considered was based on the geometry of the Swiss seismological network geometry with events in the magnitude range of 3-5.5 (Figure 5). As the dataset generation provided FAS of signal and noise, a signal-to-noise ratio >3 was imposed. 50 stations observing 100 events were considered which resulted in hypocentral distances up to 200 km.

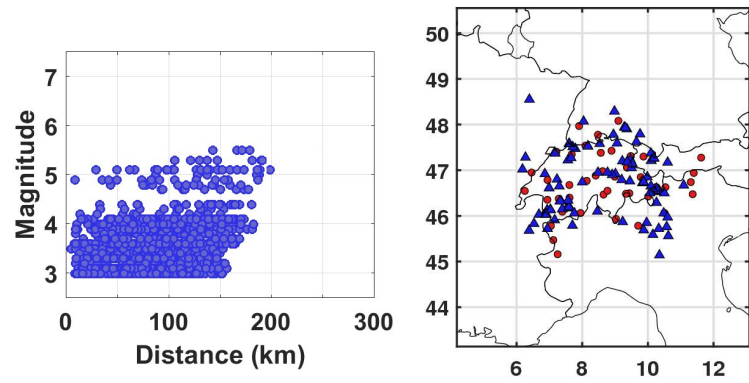
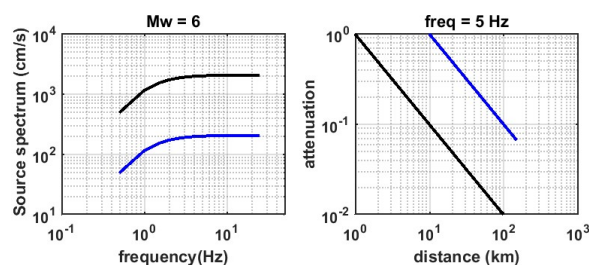


Figure 5 : Magnitude-distance distribution of the synthetic dataset (left). Spatial configuration of the seismic network (triangles) and generated events (circles) (right).

3. How to compare results from parametric and non-parametric approaches

As implied in the previous sections, the direct and consistent comparisons of general GIT outputs is not possible before a homogenization process of the parametric/non-parametric outputs obtained from each approach. As reminder, the complete non-parametric approaches delivers source terms as explicit functions of frequency, attenuation terms as function of the hypocentral distance $A(r)$ for each frequency point, and site amplifications as functions of frequency. While the parametric approach delivers directly predefined model parameters for either the source (i.e. Moment Magnitude M_w , corner frequencies f_c , and stress drops $\Delta\sigma$) or attenuation (quality factor Q , geometrical spreading factor γ). Based on this, two levels of comparisons were established.

A first level comparisons was carried out on non-parametric curves where the results of the parametric approaches were combined together to get the full non-parametric source information. Similar treatment was done for the attenuation curves. On the comparisons of non-parametric curves, it is worth mentioning that the results of the of the non-parametric inversions schemes for the source correspond to sources shifted at the reference distance (R_{REF}) used in the inversion scheme. This choice of reference distance not is not directly implied in the parametric approaches, but it is systematically considered as 1km. So a scaling of the source spectra with R_{REF} was needed for comparable results. The latter concept of scaling was similarly applied for attenuation as the non-parametric results consider $A(r = R_{ref}, f) = 1$. A schematic illustrative comparison is shown in Figure 6, where the need to scale the source and attenuation terms by R_{ref} (which was taken 10 km in the plot) is shown by the difference between the black (with $R_{ref} = 1$ km) and blue (with $R_{ref} = 10$ km) curves.



	Research and Development Program on Seismic Ground Motion	Réf : SIGMA2-2019-D3-030/1 Version : 1
--	--	---

Figure 6 : illustrative figure showing the difference in scaling observed/assumed in non-parametric results. The blue curves represent non-parametric approach results with a considered reference distance of 10 km, while the back curves shows unscaled true curves.

A Second level comparison was done on the obtained physical parameters from each approach. For instance, comparisons between source parameters were carried out on M_w , f_c and $\Delta\sigma$. To obtain these parameters from non-parametric source curves, we had to fit the source spectra with the Brune's (1970) model:

$$\Omega(f) = \left(\frac{2R_{\theta\phi}}{4\pi\rho\beta^3} \right) \left(\frac{(2\pi f)^2 \cdot M_0}{1 + \left(\frac{f}{f_c}\right)^2} \right) \quad (3)$$

where M_0 is the seismic moment and f_c the corner frequency of earthquake, $R_{\theta\phi}$ the source radiation pattern, assumed to be constant ($R_{\theta\phi} = 0.55$ for S-waves, Boore and Boatwright 1984), ρ the density, β the S-wave velocity of the medium at the source and v_s is the average S-wave velocity along the path (assuming that $\beta = v_s = 3.5$ km/s and $\rho = 2800$ kg/m³, as taken in several studies (Drouet et al., 2010; Bindi et al., 2017...)). The values of the stress drops were determined from as following the Brune's stress drops:

$$\Delta\sigma = \frac{7}{16} M_0 \left(\frac{f_c}{0.37v_s} \right)^3 \quad (4)$$

The attenuation term, accounting for path effects, involves anelastic decay and geometrical spreading so non-parametric attenuation functions were fitted with this simple model as it follows:

$$A(r, f) = \exp\left(-\frac{\pi r f}{Q_0 f^\alpha v_s}\right) \cdot \left(\frac{R_{REF}}{r}\right)^\gamma \quad (5)$$

where α is the frequency-dependence quality factor $Q = Q_0 f^\alpha$ and γ is the coefficient of the geometrical spreading (in theory 1 for pure body waves, 0.5 for pure surface waves).

This process of post-fitting was done in a consistent manner for all non-parametric results, and the choice of these simple models allowed consistent comparisons between the inverted parameters from the different approaches. The attenuation model derived is in all cases representative over the distance range observed in the dataset, and is not necessarily representative of the attenuation characteristics outside the investigated region (shorter or larger distances).

4. Methods check with a simple synthetic dataset (Sanity check)

The main motivation to examine a synthetic dataset was to evaluate performance of each GIT scheme as sort of sanity check before starting the inversions on real datasets. This helped to avoid all kinds of ambiguities in results that could make the interpretations difficult. Briefly, the synthetic dataset considered Brune's model for the source part with a homogenous attenuation structure of a quality factor $Q=600$ (frequency-independent). The reference site was also indicated in advance so that all the inversions constrain the same reference site (the reference site code for the synthetic was PAT4 which had a flat zero amplification).

The results from different inversion schemes on the synthetic dataset were leading generally to correct parameters values used in the synthetics. The 1-to-1 plot of the output magnitudes versus input magnitudes M_w indicate that the inversions are leading around the true solution for the M_w (Figure 7). Also, comparing the inverted corner frequencies within the range [0.3-10 Hz] with inverted M_w showed that obtained stress drops are varying within the range of 30-60 bars between the different approaches (Figure 7). These results seem to be acceptable for the source parameters as the correct values of stress drops used in synthetics generation was 50 bars. Regarding the attenuation values obtained by different teams, they were converging in an acceptable range to the true values of attenuation parameters (Table 2), except for one inversion which showed a solution of the attenuation parameters (e.g. $Q_0 = 220$) which is a bit far from the true values when compared individually. Site terms inverted were showing a nice convergence to the correct site amplifications used. An example results for 3 sites were shown in (Figure 8). Finally, this test of the inversions on such a simple dataset sounded a good check and allowed some code adjustments from inversions that was helpful to continue the exercise.

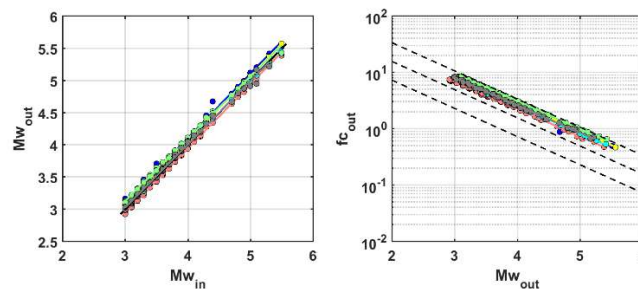


Figure 7 : synthetic dataset source results: left) the 1:1 plot of the of the M_w obtained from inversions (M_{wout}) with respect to the input Magnitudes values provided (M_{win}). right) The stress drops distributions resulting from the different approaches versus the inverted M_w values.

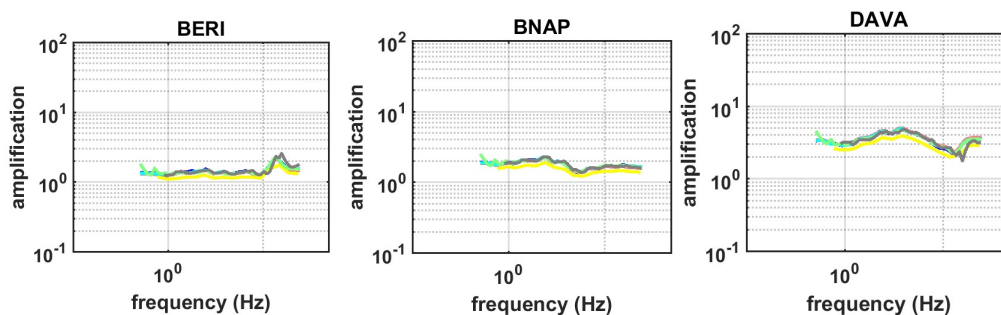


Figure 8 : example comparisons of site amplifications obtained from different approaches for three different sites, showing a good retrieval of the correct site amplifications.

Table 2 : This table summarizes the mean estimations of the attenuation parameters from different inversions

inversion	Q_0	α	γ
synthetics	600	0	1
inv: 01	532,9992433	0,06674366	1,024279613
inv: 02	220,0887375	0,355561939	0,761628709
inv: 04	555,87	0,03	0,99
inv: 05	539,0718591	0,041877481	1,000036073
Inv: 06	504,6135	0,056542	0,97944

	Research and Development Program on Seismic Ground Motion	Réf : SIGMA2-2019-D3-030/1 Version : 1
--	--	---

Inv: 07	514	0,05	0,983555
---------	-----	------	----------

5. Results on real datasets:

5.1. Choice of the reference sites in each dataset:

Initially the benchmark had two iterations, a first iteration where the inversions were done in a free way with no indications about specific choices (e.g. reference sites and conditions). The first iteration resulted in a significant variability for the site terms, and it was decided to fix all reference sites in a second iteration. So in order to reduce the possible origins of variability in the results, we managed to fix the same reference conditions in all inversions for the same dataset. Since the proper choice of reference sites oftently requires apriori knowledge about site geological conditions, we managed to constrain the inversions by choosing characterized site in each of the three real datasets. We chose sites that correspond to rock geological conditions and associated with high V_{S30} values and having recorded a significant number of events in the dataset. Based on this, we proposed to consider each of the following stations with their responses to constrain the inversions:

- OGCH site in the French dataset.
- LSS site in the Central Italy dataset

For the Japanese dataset, we considered the reference site ‘YMGH01’ that was also considered in a previous work (Nakano et al., 2015). Note that to estimate and impose in our inversions the site responses, we performed 1D-SH numerical simulations using the provided velocity profiles of the characterized stations.

5.2. French dataset results:

The aim behind the present work was to observe the possible differences in results that may happen due to the different possible implementations of inversions. To address this, we had to perform the two level comparisons (non-parametric and parametric) and try to understand the possible origins of any differences. The comparisons start on the French dataset proposed within GITEC, as it was the smallest dataset in terms of amount of data recorded. The regional sparsity observed in the dataset, having source–site distances spreading over a 20-300 km range, implied strongly varying attenuation curves at large distances. The results of the different inversions were combined and compared.

For each event in the dataset, the acceleration source spectra from non-parametric approaches, scaled with the considered reference distance, were compared to the Brune’s model resulting from parametric inversions. Figure 9, shows an overall comparison of the source spectra trying to identify the possible of a systematic over-prediction of the plateau level by one approach compared to the other. The non-parametric approaches 01 and 02 along with the parametric approach of 06 were showing on average a consistent level of source spectra plateau while the other two approaches of 04 and 07 proposed higher average levels. This average vertical shift observed in the source spectra resulting from each inversion results, will have a clear effect in the estimations of the source physical parameters.

As the estimation of the physical parameters of the seismic sources are one of the main reasons behind applying the inversion techniques and that is necessary for many applications, we present the comparisons of the source parameters determined from these inversions. As mentioned before, a post-fitting procedure was performed on the non-parametric source spectra to estimate the M_w and f_c and

	<p style="text-align: center;">Research and Development Program on Seismic Ground Motion</p>	<p>Réf : SIGMA2-2019-D3-030/1</p>
		<p>Version : 1</p>

consequently $\Delta\sigma$ using always the Brune's point source model. In Figure 10 (a), the resultant one-to-one plots of the inverted moment magnitudes (M_w) with respect to provided local Magnitudes (ML) in the catalogues are shown. As several studies and efforts are being made on the conversion relation between ML and M_w (Munafò et al., 2016; Malagnini and Munafò, 2018), it would be indicative noting that GIT results would support the general direction of these studies as it provides an estimation of the M_w -ML relation. Moreover, the overall trend that can be inferred, despite the different estimations of M_w , shows that larger ML values overestimate the M_w as coming from GIT results. This means that generalized inversions propose that the relation between M_w and ML can be considered as $n:m$ (where $n < m$) which will show a lower slope than the 1:1 relation. To add, the estimated f_c - M_w distribution showed comparable results from the inversions of 01, 02, and 06 while the inversion schemes of 04 and 07 have shown higher estimated f_c (Figure 10-b). The shift in the f_c range obtained was accompanied by remarkable differences in the stress drops for the French dataset. For example, Figure 10 (c) shows clearly the differences in the estimated $\Delta\sigma$ where approaches 01, 02, and 06 give values in the range of 0.1 to 10 bars with a mean $\Delta\sigma$ around 1 bars while the approaches 04 and 07 result in $\Delta\sigma$ values in the ranges [1-100bars] and [10-1000 bars] with mean around 10 respectively. Compared to the results found in (Drouet et al., 2010) on the same dataset, the results of the 01,02, and 06 show a factor of 10 lower for the mean $\Delta\sigma$ while the results of 07 show a factor of 10 higher. The results from the different implementations of GIT, considering the same reference conditions (as much as possible), resulted in a factor of 10 of difference for the stress drops around the expected values. To add, the dependence of $\Delta\sigma$ on M_w could not be inferred clearly as most of the data is ranging within local magnitudes 3 to 4.

To compare the attenuation terms obtained, Figure 11 shows the attenuation curves between 0.5 Hz and 25 Hz. This figure highlights the main differences in the attenuations obtained from a non-parametric approach compared to those obtained from a parametric model. The attenuation obtained from the non-parametric inversions show a significant change in slope of the attenuation for distances beyond 10 km for the lower frequencies, a fact that cannot be observed directly using a parametric model since it embeds an assumption on attenuation and its distance dependence of parameters. After fitting the non-parametric attenuation curves with simple models of attenuation and comparing them to the results obtained from parametric inversions, the results are provided in Table 3. The parameters' values show comparable estimations for the quality factor Q_0 in the range 200-350, for its frequency dependence α in the range 0.3-0.5 and for the geometrical spreading γ within the range 0.9-1.2.

As for the site responses, an overall comparison of the average amplifications could be helpful to identify the possible differences in the results (Figure 9). The inverted site amplifications from the different inversions seem to be consistent, comparable and having an overall average around 2. It could be indicated that the high frequency amplifications is showing a decay in the parametric inversion results (04 ,06 and 07) that does not appear to be clear for the non-parametric results (01 and 02) in the French dataset case. The latter observation is accompanied by the presence of a high-frequency-sloped trend of the source spectra resulting from non-parametric GIT that does not coincide with Brune's model used in parametric GIT. Thus, a main difference appears here in the high frequency range as a form of additional attenuating effect. This additional effect looks to be more expressed on the source part in non-parametric GIT while for parametric GIT this term propagates into estimated site amplifications (at least in the comparison results of the French data).

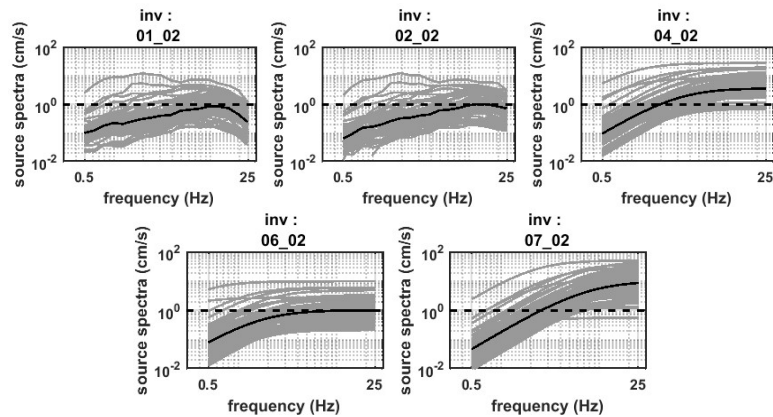


Figure 9 : an overall comparison of the source spectra obtained from the different inversions (indicated on top of each sub-figure) showing the average of all spectra (bold black).

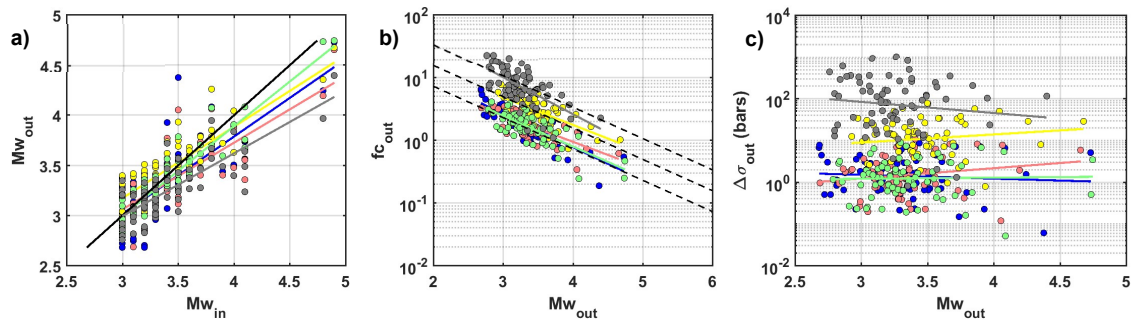


Figure 10 : French dataset source results: a) the 1:1 plot of the of the M_w obtained from inversions (M_{wout}) with respect to the ML values provided (M_{win}). b) The distribution of the corner frequencies f_c versus M_w estimated from inversions, the dashed lines are the stress drop lines of 1, 10 and 100 bars. c) The stress drops distributions resulting from the different approaches versus the inverted M_w values.

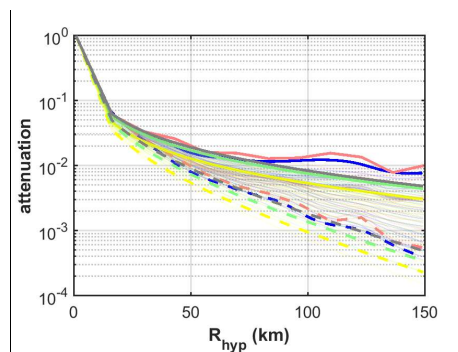


Figure 11 : the figure shows the attenuation curves obtained from each inversion scheme and plotted as function of hypocentral distance showing the curves $A(R, f=0.5 \text{ Hz})$ (lines) and $A(R, f=25 \text{ Hz})$ (dashed-lines).

Table 3 : This table summarizes the mean estimations of the attenuation parameters from different inversions

Inversion	Q_0	α	γ
inv: 01	277,6388064	0,509366052	1,259564317
inv: 02	279,6586679	0,480897622	1,240072182
inv: 04	341,73	0,31	1,07
inv: 06	236,6774	0,44736	1,0053

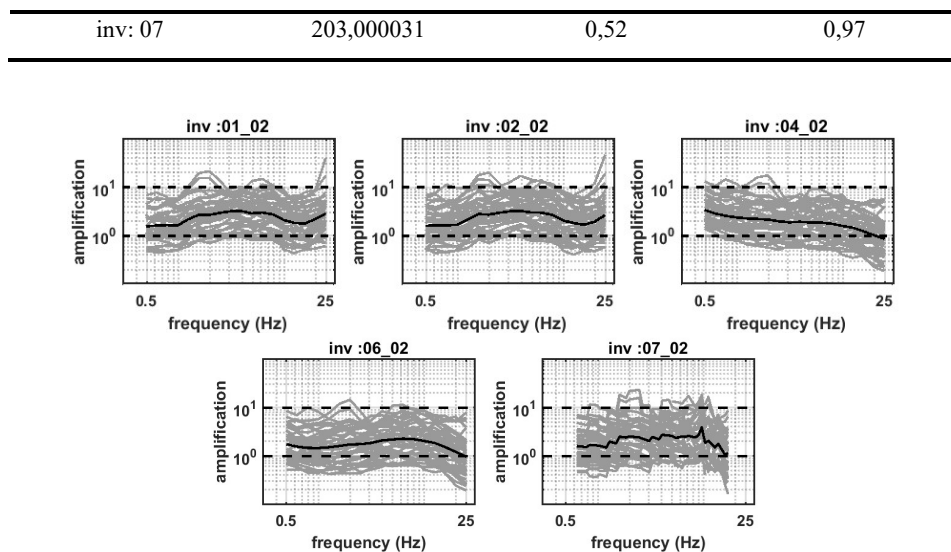


Figure 12 : an overall comparison of the site amplifications obtained from the different inversions (indicated on top of each sub-figure) showing the average of all sites (bold black).

5.3. Central Italy dataset results:

For the Italian dataset, the inversions were also performed and the systematic comparisons for the source, attenuation and site terms were established. It would be worth mentioning that the Italian dataset (Bindi et al., 2017; Pacor et al., 2016) had a significant difference in the amount of data compared to the French dataset (Drouet et al., 2010). The sites were recording tens of events and the seismic sources were perfectly recorded. Most probably, this allowed having, on average, comparable results for the source, site and attenuation terms. Figure 13 shows the overall comparison of the source spectra obtained from the different approaches, indicating a consistent mean high-frequency plateau at 1 to 2 cm/s.

The comparisons for the event parameters are shown in Figure 14, showing the Mw-ML plots that indicate, similar to the French dataset results, an overestimation by the local magnitudes ML of the Mw resulting from the GIT results. The results in terms of $\Delta\sigma$ show a mean value around 10 bars distributed between 1 and 100 bars. These results conform with the previous findings and studies on the central Italy data (Bindi et al., 2009; Ameri et al., 2011; Bindi et al., 2017), where the estimated $\Delta\sigma$ was generally in the ranges of 1 to 100 bars.

Then, comparing the attenuation terms in a similar way as in the previous section (5.2), we could visualize that the overall attenuation characteristics estimated from the different approaches. The results appear to be comparable, except for the results of '04' which proposes, somehow, a lower attenuation. Though the attenuation characteristics seemed to be comparable, the comparisons in terms of the parametric values and models showed a significant difference (Table 4). The single comparisons of the attenuation parameters (e.g. Q_0 alone) shows a wide difference between the different approaches' results (from ~ 45 up to ~ 350), but when comparing the whole set of estimated attenuation parameters (i.e. Q_0 , α and γ) we can better understand the attenuation characteristics. This observation could be interpreted by the simplicity of the attenuation model that is used, that is either the non-parametric curves $A(r,f)$ excluding all possible depth dependences of the attenuation or the standard simple parametric model used to evaluate the attenuation. Also, the used attenuation models assume a homogenous Q distribution in the studied region, which could also be rising some instabilities in the

Q -values determinations. Consequently, the fact that we are fitting very simplified models to data subject to real complex attenuation characteristics can lead to instability in the results of the model parameters. For example, the study of (Ameri et al., 2011) provided an estimation of attenuation parameter (very low $Q_0 \sim 23$) in the central Italy region but considering only data spanning the distance range up to 50 km. On the contrary, expanding the distance range of the dataset allows us to better estimate the attenuation characteristics of the crust, in comparison with the results of Bindi et al., (2017) where the same region under study provided higher Q_0 values ($Q_0 \sim 240 > 23$). To summarize, the parametric models can lead to different estimations of the crustal attenuation parameters depending on the distance range where these models fit to the data and the obtained parametric models associated with lower values of the Q_0 could fit the data better in the short distance range.

Addressing the comparisons on the site terms, the overall view of the site amplification estimation appears to be comparable between the different approaches for frequencies below 10 Hz (Figure 16). The amplification for all sites coming from each inversion show a mean value between 1 and 10 generally. Individual site comparisons and estimations will be addressed in the following paragraph. Beyond 10 Hz, a difference in the high frequency slope can be clearly seen between non-parametric ('01', '02' and '05') and parametric approaches ('04' and 06). These differences are found to be consistent when compared with the source spectra compared obtained by the same approaches. It appears to be that parametric approaches (that assumes a Brune's model for the source) have higher slopes for the site terms. On the other hand, non-parametric approaches applied on the same dataset propose instead a high frequency decay for the source spectra.

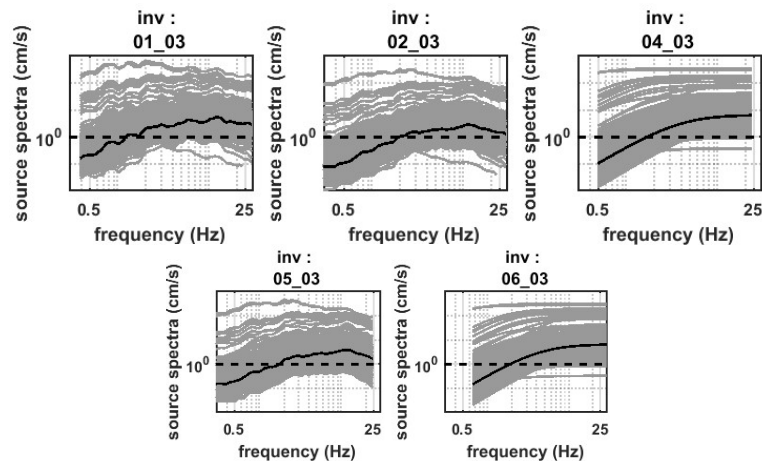


Figure 13 : Italian dataset results, an overall comparison of the source spectra obtained from the different inversions (indicated on top of each sub-figure) showing the average of all spectra (bold black).

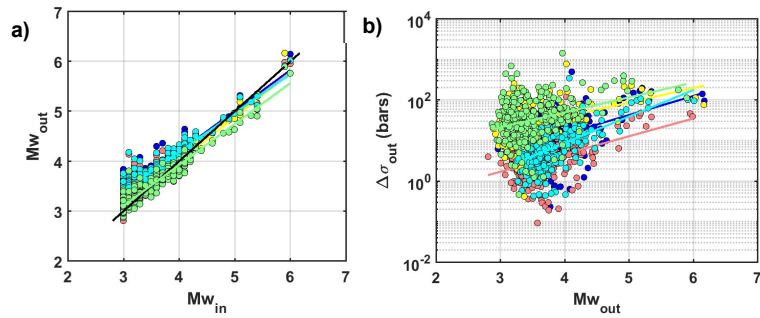


Figure 14 : Italian dataset results: a) the 1:1 plot of the of the M_w obtained from inversions (M_{wout}) with respect to the ML values provided (M_{win}). b) The stress drops distributions resulting from the different approaches versus the estimated M_w values.

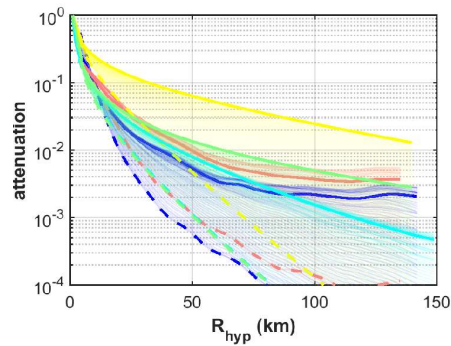


Figure 15 : The figure shows the attenuation curves obtained from each inversion scheme and plotted as function of hypocentral distance showing the curves $A(R, f=0.5 \text{ Hz})$ (lines) and $A(R, f=25 \text{ Hz})$ (dashed-lines).

Table 4 : This table summarizes the mean estimations of the attenuation parameters from different inversions

Inversion	Q_0	α	γ
inv: 01	358,0420859	0,39717548	2,225504427
inv: 02	80,62358306	0,684653658	1,244850607
inv: 04	56,13	0,59	0,56
inv: 05	45,5950769	0,74378299	1,008166425
inv: 06	98,9786	0,45512	1,0268

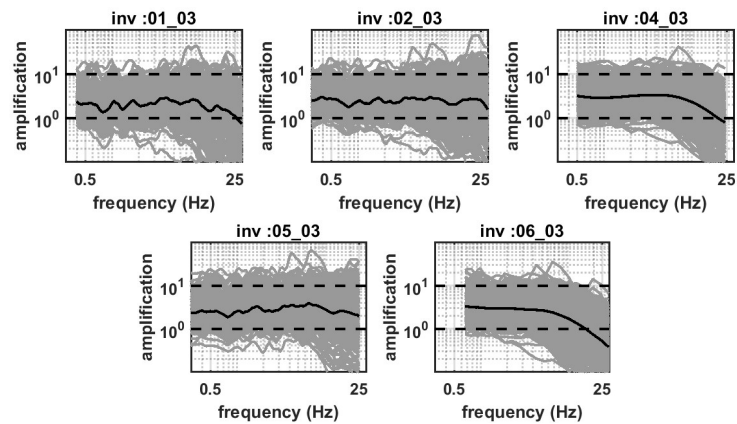


Figure 16 : Central Italy dataset: An overall comparison of the site amplifications obtained from the different inversions (indicated on top of each sub-figure) showing the average of all sites (bold black).

5.4. Japanese dataset results:

Performing the inversions on all of the Japanese regions, without taking into account the regional dependence of attenuation characteristics, was one of the initial objectives of this work. This aimed to show the possible impact of such a step on the source, attenuation and site terms results. The overall comparisons of the source spectra showed a higher plateau level of the Brune’s model resulting from approach ‘06’ inversions compared to those obtained by the non-parametric approaches. For example, Figure 17 shows an example comparison for two source spectra obtained for two events where the source spectra obtained differ significantly. These differences in the source spectra lead to different estimations of the source parameters. Figure 18, show that though Mw values are somehow comparable to each others, the result stress drops show significantly higher values to those found , for example, in Nakano et al., (2015). This difference can be explained as effects of the variations of the attenuation characteristics between the different Japanese regions.

In Figure 19, the attenuation characteristics obtained from different approaches are compared. Attenuation curves from different inversions appear to have some differences in the low frequency curves, where these differences decreased at high frequencies. Attenuation parameters presented in Table 5 show different values of the physical parameters obtained from inversions. Observing this and relating it to Figure 19, the inconsistency between the attenuation parameters from different inversions could be originating from the fact that a single attenuation model was fitted to regions where attenuation characteristics widely varies. Consequently, the higher source spectra predictions by the inversion scheme of ‘06’, the overall comparisons of site terms showed that ‘06’ inversions had provided site terms with a slightly lower average. This could be explained by the trade-off between source and sites.

Figure 20 shows example comparisons of two inverted site responses obtained from 3 different approaches. The results ‘06’ show slightly lower site amplifications, which would explain the relatively higher source spectra by the same approach ‘06’. Mainly, we suggest that due to regional dependence of attenuation, possible site-source trade-offs might happen (as the case of parametric approach results presented in the text) or source attenuation trade-offs that can leads to overestimate or underestimate the source parameters and spectra.

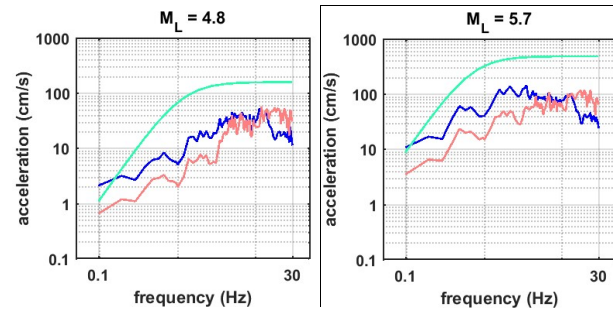


Figure 17 : Example comparisons for individual source spectra from the different inversions of two events (a-left: 1996-08-11 and b-left: 1996-08-11). The figures to right show the stations (triangles) recording the corresponding event (circles).

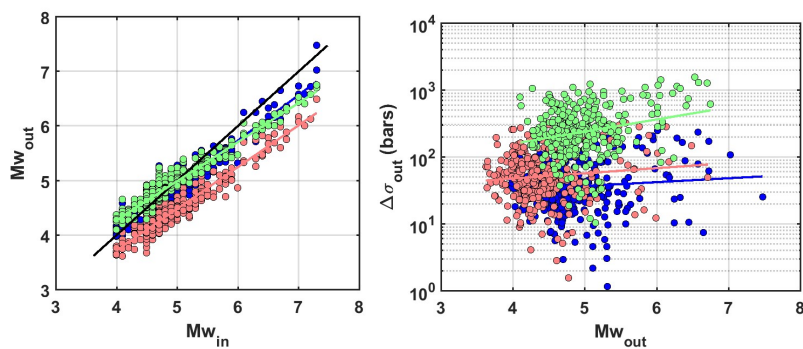


Figure 18 : Japanese dataset results: a) the 1:1 plot of the of the Mw obtained from inversions (Mwout) with respect to the ML values provided (Mwin). b) The stress drops distributions resulting from the different approaches versus the estimated Mw values.

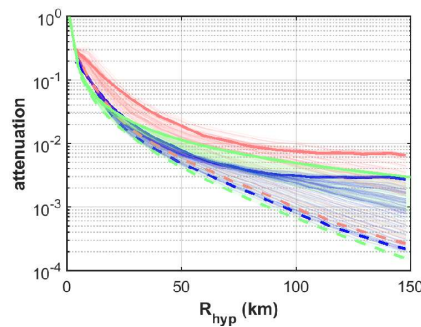


Figure 19 : The figure shows the attenuation terms obtained from each inversion scheme and plotted as function of hypocentral distance showing the curves $A(R, f=0.5 \text{ Hz})$ (lines) and $A(R, f=25 \text{ Hz})$ (dashed-lines).

Table 5 : This table summarizes the mean estimations of the attenuation parameters from different inversions

Inversion	Q_0	α	γ
inv: 01	390,3320808	0,390083829	1,346205381
inv: 02	194,4408758	0,602007166	1,061893099
inv: 06	511,9333	0,26475	1,1293

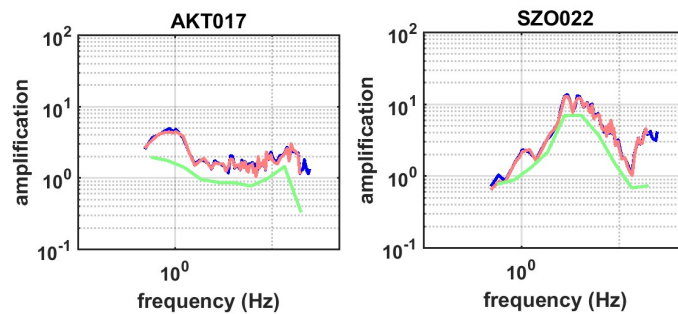


Figure 20 : Two example site amplifications obtained, showing the difference obtained from the parametric approach and the two other non-parametric approaches.

6. Inter-methods variability assessment

As one of the objectives of the benchmark was to investigate the uncertainties associated on the GIT results, we tried to estimate the variability in the results obtained by the different approaches on each dataset. Since the estimation of uncertainty on a specific parameter needed a sufficient number of estimations of the parameter, we simply address the variability in the results by computing the standard deviations obtained from the results of the different approaches. For instance, we assessed the variability, based on the performed inversions, on the non-parametric curves of the source, attenuation and site terms for each frequency. Then, it was interesting to see how and by how much the variability on the non-parametric curves can propagate to the estimations of the physical source parameters.

To add, in order to assess the possible relation of the variability of the results within the dataset to data, we defined the distance coverage and the azimuthal coverage terms. The distance coverage defines the difference between the maximum and minimum hypocentral distances at which an event has been recorded or a site has been recording. Similarly, we defined azimuthal coverage as the difference between the maximum and minimum event-site azimuth over which an event had been recording. Then we tried to assess the variation of event and site results as function of these terms. To add, comparing the variabilities with variation of depths of events and input magnitudes (local magnitudes) was done.

6.1. French dataset case :

Two example results for the events of 2003-10-16 and 2004-05-14 are displayed in Figure 21, where the source spectra from all approaches are compared showing the differences observed of the plateau level. The two non-parametric approaches of '01' and '02' seem to give consistent inverted source spectra comparable to the Brune's model by approach '06' which is not consistent with the results of approaches '04' and '07'. To quantify the variability between the different source spectra obtained, the standard deviation in logarithmic scale was computed (\log_{10}) for each source spectrum. The results are summarized and displayed in Figure 22. The variability observed appears to be increasing from 0.2 at lower frequencies to exceed 0.7 at frequencies beyond 15 Hz.

This large variability on the source spectra was implied by a large variability on the source parameters $\Delta\sigma$ and f_c estimated using the Brune's model but not on M_w (Figure 23). Figure 23 presents the estimation of the variability of the source parameters applying the standard deviation normalized by the mean for each event's parameters, showing the percentage of variation around the mean. The statistics for the French dataset shows very low inter-methods variability on the magnitude M_w as

compared to that observed for the f_c and $\Delta\sigma$ parameters, with no clear trend observed with distance and azimuthal coverages.

Regarding the results on site terms, the estimation of the variability for all sites for in the French dataset are presented in Figure 22. The variability in the estimation of the site terms appears to be very low compared to that observed on the source part, as standard deviation does not exceed 0.2 for all sites. The fact the resulting variability on the site amplifications from different approaches sounds very interesting as generalized inversions can be considered as a reliable tool for site amplification estimations.

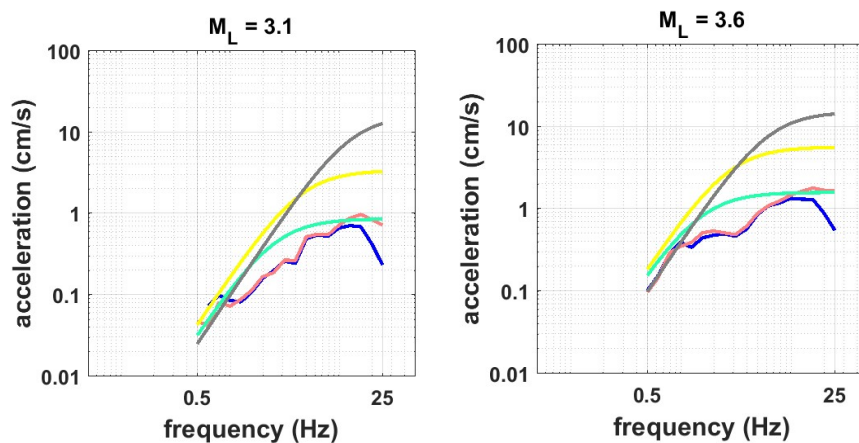


Figure 21 : Example comparisons for individual source spectra from the different inversions of two events (a-left: 2003-10-16 and b-left: 2004-05-14).

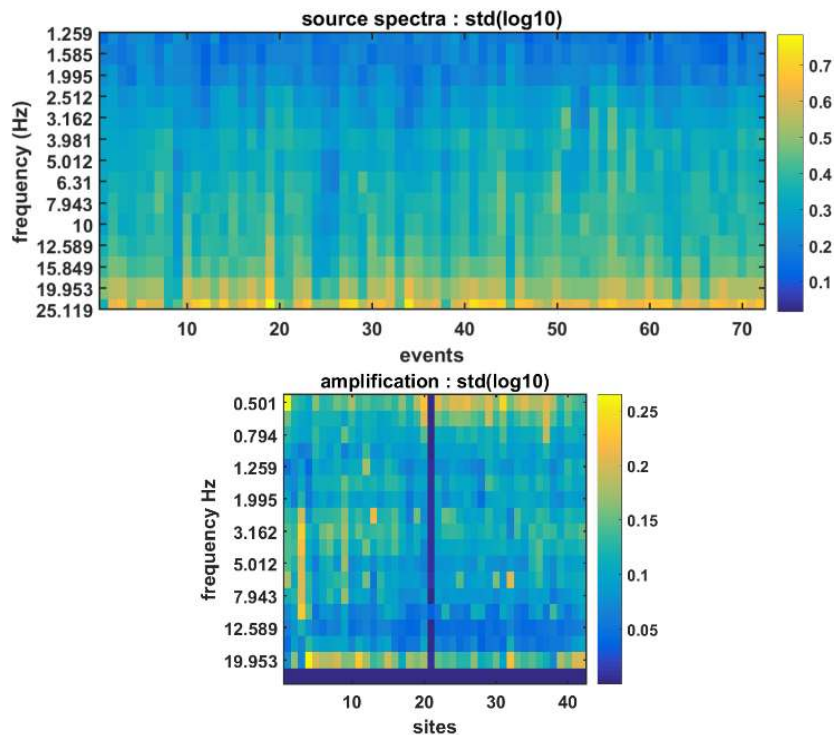


Figure 22 : The estimations of the variability as standard deviations in \log_{10} at each frequency for source spectra and amplifications obtained after inversions.

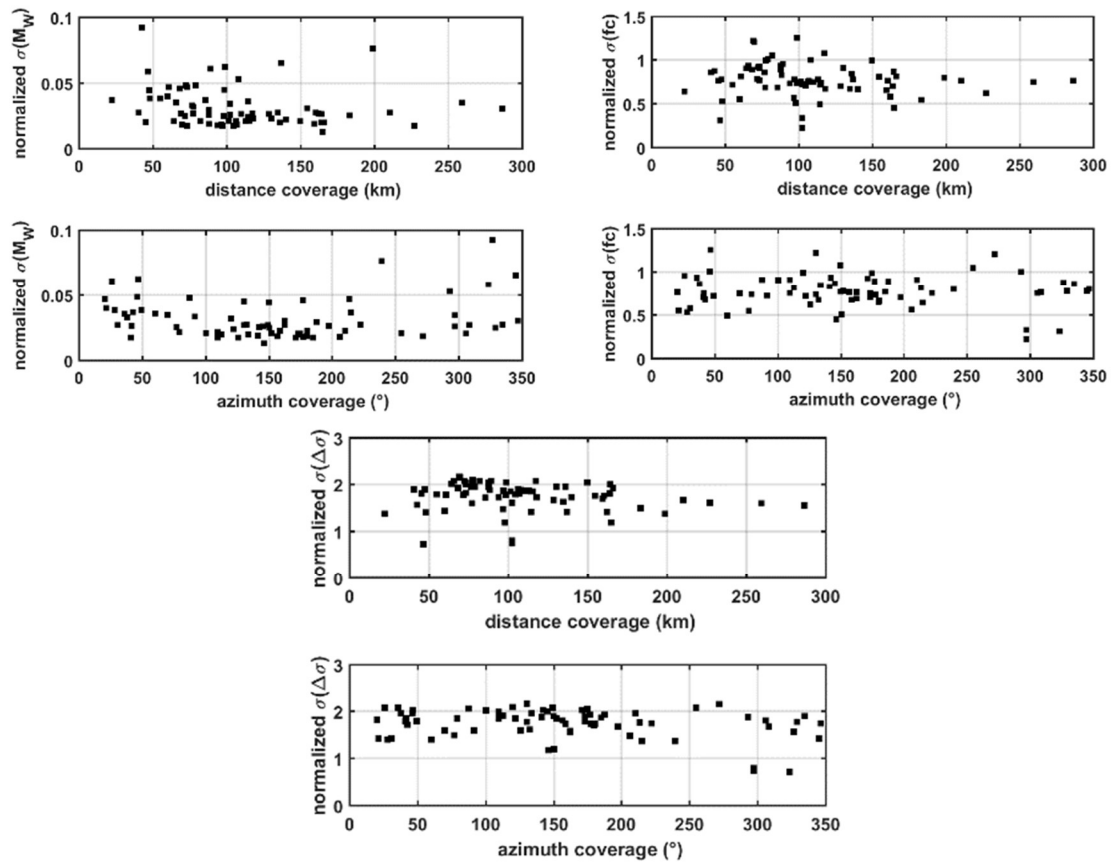


Figure 23 : estimated variability on each of the source physical parameters M_w , f_c and stress drops compared to the distance and azimuthal coverages.

6.2. Central Italy dataset case :

The same methodology of comparisons is repeated for GIT results on the Italian dataset. The resulting source spectra from the applied approaches presented very consistent comparisons, where the variability on the source spectra did not exceed 0.2 over almost the whole frequency band (Figure 24). The reason behind these comparable results was probably due to the good geometry and density of the network that allowed recording each event tens or event hundreds of times. Compared to the French dataset results, these results seem to show that the redundancy in the dataset in terms of recordings is essential and helpful for generalized inversions, or in other words, the number of the recordings per event/site is high enough.

The lower variability obtained on the source spectra was accompanied by lower variability in the results of source parameters compared to that observed in the French data. As shown in Figure 25, the M_w values show the lowest variabilities (less than 5%) which appears to decrease with increasing depth and ML. Though lower variabilities on f_c and $\Delta\sigma$ compared to the French data results were observed, the variability on these two parameters remains high (exceeds 50%) accompanied by no observation of a tendency to decrease or increase with event depths or ML (or even distance or azimuthal coverages that was displayed within this text).

As for the variability in site amplifications displayed in Figure 24, again the results from different approaches resulted in a low variability around 0.2 (in log10) over almost all the frequency band.

These results supports the conclusions made on the robustness of site terms obtained from generalized inversions. It also important to note here that these the French and Italian dataset were similar in terms of regional variations or dependence of the attenuation effects. In addition, that is why it was important to investigate for the impact of neglecting significant regional attenuation differences in a generalized inversion and what could results in source and site terms.

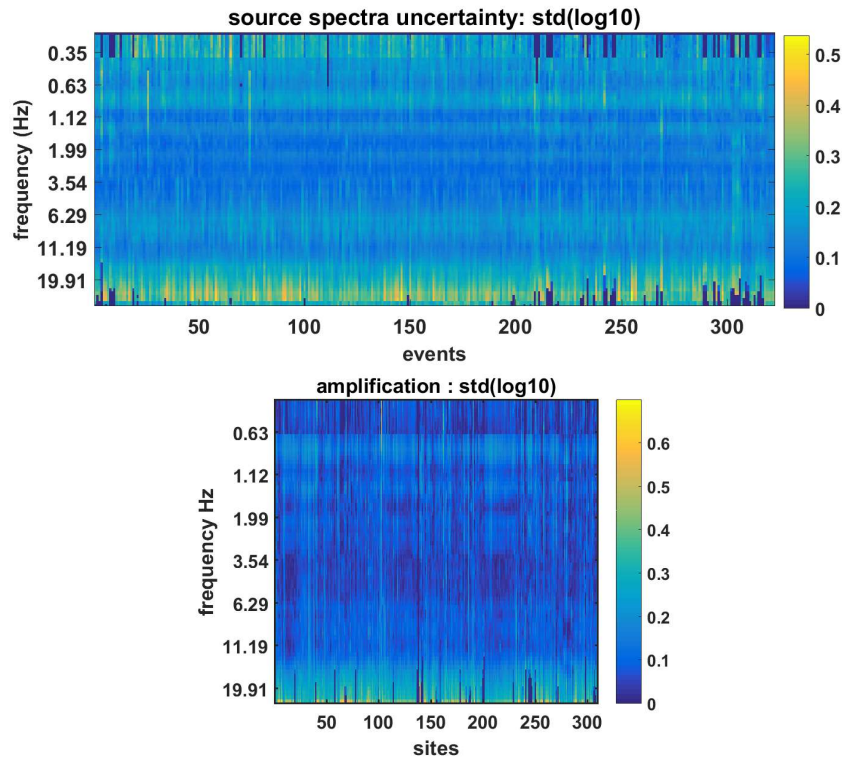


Figure 24 : The estimations of the variability as standard deviations in log10 at each frequency for source spectra and amplifications obtained after inversions.

6.3. Japanese dataset case:

For the Japanese dataset inversions, only 3 different inversions were done. Though this would not fully reflect the variability that could result from applying generalized inversions on a dataset of strong regional dependence of attenuation properties, we present hereafter the results following comparisons methodology in the previous sections. Noting the at least two additional inversions on this dataset are still being prepared on this dataset, that would give a clearer idea of the resulting variability. Figure 26 shows the standard deviation computed on the source spectra obtained from each inversion as well as for the amplifications for each site. Further statistical analyses can be provided and updated when including the results from additional inversions.

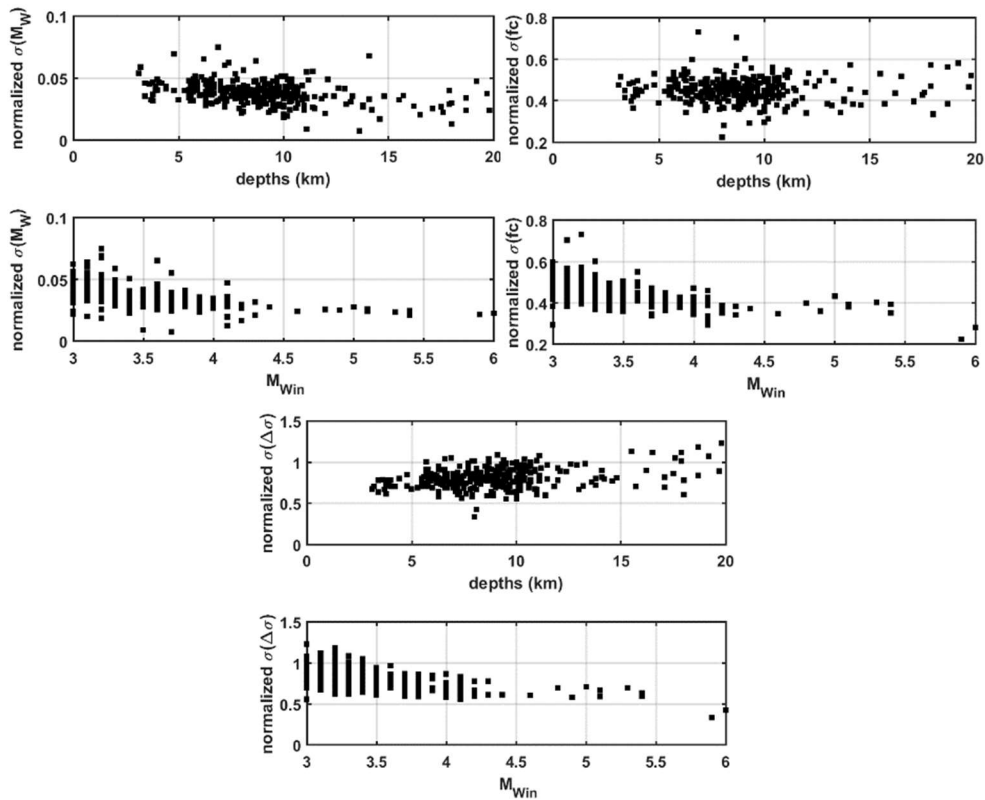


Figure 25 : estimated variability on each of the source physical parameters M_w , f_c and stress drops compared to the input magnitudes and depths of events.

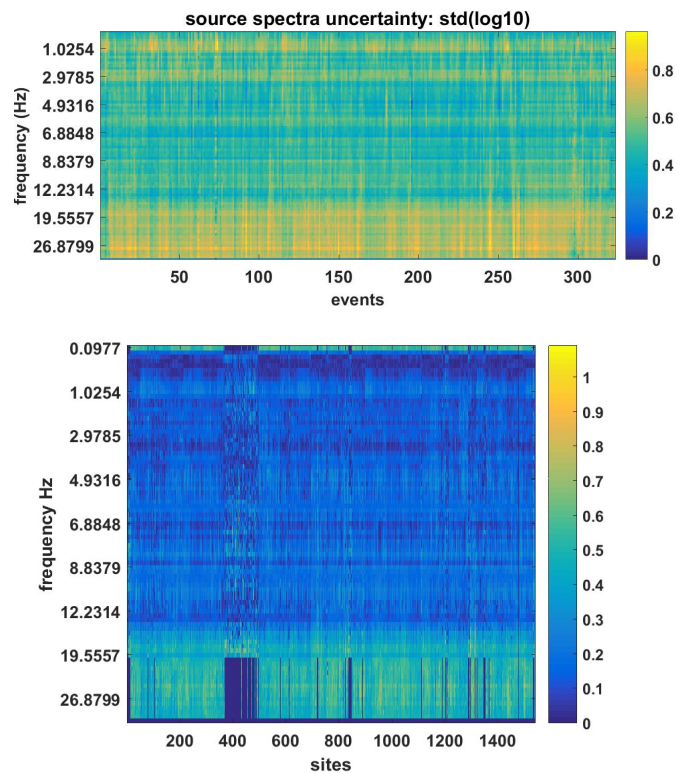


Figure 26 : The estimations of the variability as standard deviations in \log_{10} at each frequency for source spectra and amplifications obtained after inversions.

	<p style="text-align: center;">Research and Development Program on Seismic Ground Motion</p>	<p>Réf : SIGMA2-2019-D3-030/1</p>
		<p>Version : 1</p>

7. Summary and conclusions:

The benchmark carried out on generalized inversion techniques considered three real datasets prepared and used in previous publications. In addition, a simple synthetic dataset was considered to check the convergence of all methods to the right solution. The inversions carried out served most of the initial benchmark objectives. The chosen datasets for the benchmark had different configurations and characteristics which could be attributed to some of the differences observed in the results of inversions. First, the inversions on the French dataset, with its large sparse spatial distribution of events and sites, and low number of recordings resulted in significantly different source spectra among participating teams. However, the estimations of the source parameters for the French dataset showed comparable values for the magnitudes (M_w) unlike the corner frequencies and stress drop results. On the other side, attenuation characteristics obtained from different inversions resulted in similar attenuation properties up till 250 km. The site responses estimated for the French dataset, despite the discrepancies in the source terms, are consistent and show the lowest inter-method variabilities. For the Italian dataset, the variability observed on source spectra was much lower and was translated by a lower variability on the source parameters. However, the corner frequencies and stress drops showed higher variabilities than M_w between the different methods. Attenuation and site responses showed lower variabilities, in consistency with the results of the French dataset. For the Japanese dataset, discrepancies on the source-attenuation part between the two non-parametric approaches were observed, which also showed difference to those obtained from a parametric approach.

The main observations and conclusions summarize as follows:

- The M_w source parameter shows less variability among the different approaches than the corner frequency (f_c) and stress drops ($\Delta\sigma$).
- The attenuation characteristics from different approaches are comparable (when comparing attenuation curves), but when addressing the parametrization, individual attenuation parameters, such as Q_0 , could not be fully reflecting the crustal attenuation in the studied region. That can be mainly attributed to the simplicity of the Q -model considered.
- Comparing the resulting variability from French and Italian datasets, data redundancy appears to be important (sufficient number of recordings per event/site).
- The site terms appears to be the terms associated with lowest variability among the different results, given that no rough assumptions are made concerning the attenuation (such as assuming that Japanese dataset is covering a region with homogenous attenuation model) or choice of reference sites.
- For the source parameters, more precisely, the M_w -ML relation from different approaches appears to be consistent.

Commenting the different approaches used (parametric/non-parametric), each approach appears to have its own merits. When having very small amount of data in a given dataset, the application of a non-parametric approach seems to be difficult. For example, the attenuation model derived in such approach can only be defined using the source-site distance points found in the dataset. Unlikely in a parametric approach, the model assumed from the beginning is calibrated through the inversion iterations to fit the recorded data characteristics.

Non-parametric GIT is accompanied by an assumption made on attenuation and source parameters defined by the reference distance ' R_{ref} '. This assumption implies that all sources are shifted at

	<p style="text-align: center;">Research and Development Program on Seismic Ground Motion</p>	<p>Réf : SIGMA2-2019-D3-030/1</p>
		<p>Version : 1</p>

this R_{ref} with attenuation starting from unity at this distance, which can be a very critical assumption when having no data in the short distance range (<50 km for example). On the other hand, a non-parametric approach appears to provide more information about regional attenuation and earthquake sources than parametric approaches as the un-modeled attenuation curves and source spectra can be visualized with less a priori assumptions. So, it is an important point to reduce a priori assumptions as much as possible to verify models adequacy.

Following the several points mentioned in the text about the reliability of earthquake spectra decomposition at high frequencies, several questions can be posed. For the first instance, one can directly propose that reducing assumptions on sources (non-parametric spectra instead of the Brune's model) could be the reason behind the high frequency discrepancies. The latter proposition can only be accepted if the inversion scheme used is stable enough and free of high frequency trade-offs. This can be followed by interpretations that address the inadequacy of the Brune's model beyond 10 Hz. For example, the study of Bindi et al., (2019) on data from central Italy proposes a source model anchored by a parameter called ' κ_{source} '. Though, the high frequency performance of the inversion schemes remains questioned. On the other hand, if the susceptibility of the non-parametric inversion schemes to trade-offs was possible, then these differences at high frequency can be possibly misleading. Thus, parametric models (especially Brune's model) could be preferred instead letting chance to trade-offs take place. The final answer to all question about high frequency performance of these methods remains not so clear and needs more investigations and tests. To conclude, the preference on either parametric or non-parametric approaches seems to be not very clear and could be case dependent based on the dataset of interest (e.g. amount of data present, etc...). However, a best practice we propose is to proceed carefully with the two approaches in parallel and compare consistently the results from the different approaches before direct application and use of corresponding results.

8. Future perspectives:

In addition to present work in this text, several questions are posed within the GITEC group that serves as several perspectives of the work:

- The fact that attenuation properties in generalized inversions play an important role (either in the case of significant regional dependencies or the instability of the Q-model parameters as estimated from inversions), a more complicated synthetic could be addressed. The synthetic dataset that could be proposed to investigate such a problematic can be taking into account some regional differences as well as the depth-dependence of attenuation.
- In addition, the question of the minimum/maximum magnitude limits below which the corner frequencies cannot be resolved, as they become no more lying in the frequency band under study.
- The high frequency discrepancies can be an interesting point to investigate instead of pushing all interpretations towards parameters which doesn't have a clear physical basis.
- Also, it could be interesting to investigate in more details the impact of the network position of a given event/site on the corresponding results, as well as the possibility to retrieve site amplifications for newly added sites within a network, having very low number of data. These questions could be addressed by the use of real or synthetic data.

	Research and Development Program on Seismic Ground Motion	Réf : SIGMA2-2019-D3-030/1 Version : 1
--	--	---

- One of the questions could also be posed is how to capture the failure of the point source assumption (Brune's model) in GIT or the radiation patterns from real data with help of synthetics.

Acknowledgements

This work is carried out within the framework of SIGMA2 program. Special thanks for all participants especially in dataset preparations from Hiroshi Kawase (Kyoto University, Japan), Francesca Pacor (INGV Milano, Italy), Daniele Spallarossa (University of Genova, Italy), Ben Edwards (University of Liverpool, England), Stephane Drouet (GEOTER, France).

References

- Ameri, G., Oth, A., Pilz, M., Bindi, D., Parolai, S., Luzi, L., Mucciarelli, M., Cultrera, G., 2011. Separation of source and site effects by generalized inversion technique using the aftershock recordings of the 2009 L'Aquila earthquake. *Bull Earthquake Eng* 9, 717–739. <https://doi.org/10.1007/s10518-011-9248-4>
- Andrews, D.J., 1986. Objective Determination of Source Parameters and Similarity of Earthquakes of Different Size, in: Das, S., Boatwright, J., Scholz, C.H. (Eds.), *Earthquake Source Mechanics*. American Geophysical Union, pp. 259–267. <https://doi.org/10.1029/GM037p0259>
- Bindi, D., Pacor, F., Luzi, L., Massa, M., Ameri, G., 2009. The Mw 6.3, 2009 L'Aquila earthquake: source, path and site effects from spectral analysis of strong motion data. *Geophys J Int* 179, 1573–1579. <https://doi.org/10.1111/j.1365-246X.2009.04392.x>
- Bindi, D., Parolai, S., Grosser, H., Milkereit, C., Karakisa, S., 2006. Crustal Attenuation Characteristics in Northwestern Turkey in the Range from 1 to 10 Hz. *Bulletin of the Seismological Society of America* 96, 200–214. <https://doi.org/10.1785/0120050038>
- Bindi, D., Spallarossa, D., Pacor, F., 2017. Between-event and between-station variability observed in the Fourier and response spectra domains: comparison with seismological models. *Geophys J Int* 210, 1092–1104. <https://doi.org/10.1093/gji/ggx217>
- Bonilla, L.F., Steidl, J.H., Lindley, G.T., Tumarkin, A.G., Archuleta, R.J., 1997. Site amplification in the San Fernando Valley, California: Variability of site-effect estimation using the S-wave, coda, and H/V methods. *Bulletin of the Seismological Society of America* 87, 710–730.
- Bora, S.S., Scherbaum, F., Kuehn, N., Stafford, P., Edwards, B., 2015. Development of a Response Spectral Ground-Motion Prediction Equation (GMPE) for Seismic-Hazard Analysis from Empirical Fourier Spectral and Duration Models. *Bulletin of the Seismological Society of America* 105, 2192–2218. <https://doi.org/10.1785/0120140297>
- Borcherdt, R.D., 1970. Effects of local geology on ground motion near San Francisco Bay. *Bulletin of the Seismological Society of America* 60, 29–61.
- Castro, R.R., Anderson, J.G., Singh, S.K., 1990. Site response, attenuation and source spectra of S waves along the Guerrero, Mexico, subduction zone. *Bulletin of the Seismological Society of America* 80, 1481–1503.
- Drouet, Cotton Fabrice, Guéguen Philippe, 2010. v S30, κ , regional attenuation and Mw from accelerograms: application to magnitude 3–5 French earthquakes. *Geophysical Journal International* 182, 880–898. <https://doi.org/10.1111/j.1365-246X.2010.04626.x>
- Drouet, S., Chevrot, S., Cotton, F., Souriau, A., 2008. Simultaneous Inversion of Source Spectra, Attenuation Parameters, and Site Responses: Application to the Data of the French Accelerometric Network. *Bulletin of the Seismological Society of America* 98, 198–219. <https://doi.org/10.1785/0120060215>

	<p>Research and Development Program on Seismic Ground Motion</p>	<p>Réf : SIGMA2-2019-D3-030/1</p> <p>Version : 1</p>
--	--	--

- Drouet, S., Cotton, F., 2015. *Regional Stochastic GMPEs in Low-Seismicity Areas: Scaling and Aleatory Variability Analysis—Application to the French Alps* *Regional Stochastic GMPEs in Low-Seismicity Areas: Scaling and Aleatory Variability Analysis. Bulletin of the Seismological Society of America* 105, 1883–1902. <https://doi.org/10.1785/0120140240>
- Edwards, B., Rietbrock, A., Bommer, J.J., Baptie, B., 2008. *The Acquisition of Source, Path, and Site Effects from Microearthquake Recordings Using Q Tomography: Application to the United Kingdom* *Acquisition of Source, Path and Site Effects from Microearthquake Recordings Using Q Tomography. Bulletin of the Seismological Society of America* 98, 1915–1935. <https://doi.org/10.1785/0120070127>
- Field, E.H., Jacob, K.H., 1995. *A comparison and test of various site-response estimation techniques, including three that are not reference-site dependent. Bulletin of the Seismological Society of America* 85, 1127–1143.
- Hartzell, S.H., 1992. *Site response estimation from earthquake data. Bulletin of the Seismological Society of America* 82, 2308–2327.
- Klin, P., Laurenzano, G., Priolo, E., 2018. *GITANES: A MATLAB Package for Estimation of Site Spectral Amplification with the Generalized Inversion Technique. Seismological Research Letters* 89, 182–190. <https://doi.org/10.1785/0220170080>
- Laurendeau, A., Bard, P.-Y., Hollender, F., Perron, V., Foundotos, L., Ktenidou, O.-J., Hernandez, B., 2018. *Derivation of consistent hard rock (1000 < VS < 3000 m/s) GMPEs from surface and down-hole recordings: analysis of KiK-net data. Bull Earthquake Eng* 16, 2253–2284. <https://doi.org/10.1007/s10518-017-0142-6>
- Malagnini, L., Munafò, I., 2018. *On the Relationship between ML and Mw in a Broad Range: An Example from the Apennines, Italy* *Short Note. Bulletin of the Seismological Society of America* 108, 1018–1024. <https://doi.org/10.1785/0120170303>
- Munafò, I., Malagnini, L., Chiaraluce, L., 2016. *On the Relationship between Mw and ML for Small Earthquakes* *Short Note. Bulletin of the Seismological Society of America* 106, 2402–2408. <https://doi.org/10.1785/0120160130>
- Nakano, K., Matsushima, S., Kawase, H., 2015. *Statistical Properties of Strong Ground Motions from the Generalized Spectral Inversion of Data Observed by K-NET, KiK-net, and the JMA Shindokei Network in Japan* *Statistical Properties of Strong Ground Motions from the Generalized Spectral Inversion of Data. Bulletin of the Seismological Society of America* 105, 2662–2680. <https://doi.org/10.1785/0120140349>
- Oth, A., Bindi, D., Parolai, S., Giacomo, D.D., 2011. *Spectral Analysis of K-NET and KiK-net Data in Japan, Part II: On Attenuation Characteristics, Source Spectra, and Site Response of Borehole and Surface Stations* *Spectral Analysis of K-NET and KiK-net Data in Japan, Part II. Bulletin of the Seismological Society of America* 101, 667–687. <https://doi.org/10.1785/0120100135>
- Pacor, F., Spallarossa, D., Oth, A., Luzi, L., Puglia, R., Cantore, L., Mercuri, A., D’Amico, M., Bindi, D., 2016. *Spectral models for ground motion prediction in the L’Aquila region (central Italy): evidence for stress-drop dependence on magnitude and depth. Geophys J Int* 204, 697–718. <https://doi.org/10.1093/gji/ggv448>
- Parolai, S., Bindi, D., Baumbach, M., Grosser, H., Milkereit, C., Karakisa, S., Zünbül, S., 2004. *Comparison of Different Site Response Estimation Techniques Using Aftershocks of the 1999 Izmit Earthquake. Bulletin of the Seismological Society of America* 94, 1096–1108. <https://doi.org/10.1785/0120030086>
- Perron, V., Hollender, F., Bard, P.-Y., Gélis, C., Guyonnet-Benaize, C., Hernandez, B., Ktenidou, O.-J., 2017. *Robustness of Kappa (κ) Measurement in Low-to-Moderate Seismicity Areas: Insight from a Site-Specific Study in Provence, France* *Robustness of Kappa (κ) Measurement in Low-to-Moderate Seismicity Areas. Bulletin of the Seismological Society of America* 107, 2272–2292. <https://doi.org/10.1785/0120160374>

	<p>Research and Development Program on Seismic Ground Motion</p>	<p>Réf : SIGMA2-2019-D3-030/1</p>
		<p>Version : 1</p>

Salazar, W., Sardina, V., Cortina, J. de, 2007. A Hybrid Inversion Technique for the Evaluation of Source, Path, and Site Effects Employing S-Wave Spectra for Subduction and Upper-Crustal Earthquakes in El Salvador. Bulletin of the Seismological Society of America 97, 208–221. <https://doi.org/10.1785/0120060076>